

# The Supercarbonate Apatite-MicroRNA Complex Inhibits Dextran Sodium Sulfate-Induced Colitis

Tadafumi Fukata,<sup>1</sup> Tsunekazu Mizushima,<sup>1</sup> Junichi Nishimura,<sup>1</sup> Daisuke Okuzaki,<sup>2</sup> Xin Wu,<sup>3</sup> Haruka Hirose,<sup>3</sup> Yuhki Yokoyama,<sup>3</sup> Yui Kubota,<sup>3</sup> Kazuya Nagata,<sup>3</sup> Naoto Tsujimura,<sup>1</sup> Akira Inoue,<sup>1</sup> Norikatsu Miyoshi,<sup>1</sup> Naotsugu Haraguchi,<sup>1</sup> Hidekazu Takahashi,<sup>1</sup> Taishi Hata,<sup>1</sup> Chu Matsuda,<sup>1</sup> Hisako Kayama,<sup>4,5</sup> Kiyoshi Takeda,<sup>4,5</sup> Yuichiro Doki,<sup>1</sup> Masaki Mori,<sup>1</sup> and Hirofumi Yamamoto<sup>1,3</sup>

<sup>1</sup>Department of Gastroenterological Surgery, Graduate School of Medicine, Osaka University, Yamadaoka 2-2, Suita City, Osaka, Japan; <sup>2</sup>Genome Information Research Center, Research Institute for Microbial Diseases, Osaka University, Yamadaoka 3-1, Suita City, Osaka, Japan; <sup>3</sup>Department of Molecular Pathology, Division of Health Sciences, Graduate School of Medicine, Osaka University, Yamadaoka 1-7, Suita City, Osaka, Japan; <sup>4</sup>Laboratory of Immune Regulation, Department of Microbiology and Immunology, Graduate School of Medicine, Yamadaoka 2-2, Suita City, Osaka, Japan; <sup>5</sup>Laboratory of Mucosal Immunology, WPI Immunology Frontier Research Center, Osaka University, Yamadaoka3-1, Suita City, Osaka, Japan

**The incidence of inflammatory bowel disease (IBD) is increasing. Nucleic acid-based medicine has potential as a next-generation treatment, but it is rarely successful with IBD. The aim of this study was to establish a microRNA-based therapy in an IBD model. For this purpose, we used microRNA-29 (miR-29) and a supercarbonate apatite (sCA) nanoparticle as a drug delivery system. Injection of sCA-miR-29a-3p or sCA-miR-29b-3p into mouse tail veins markedly prevented and restored inflammation because of dextran sulfate sodium (DSS)-induced colitis. RNA sequencing analysis revealed that miR-29a and miR-29b could inhibit the interferon-associated inflammatory cascade. Subcutaneous injection of sCA-miR-29b also potently inhibited inflammation, and it efficiently targeted CD11c<sup>+</sup> dendritic cells (DCs) among various types of immune cells in the inflamed mucosa. RT-PCR analysis indicated that the miR-29 RNAs in CD11c<sup>+</sup> DCs suppressed the production of interleukin-6 (IL-6), transforming growth factor  $\beta$  (TGF- $\beta$ ), and IL-23 subunits in DSS-treated mice. This may inhibit Th17 differentiation and subsequent activation, which is critical in IBD pathogenesis. *In vivo* experiments using a non-natural artificial microRNA sequence revealed that targeting of DCs in the inflamed colon is an exceptional feature of sCA. This study suggests that sCA-miR-29s may open a new avenue in nucleic acid-based medicine for IBD treatment.**

## INTRODUCTION

Inflammatory bowel disease (IBD) is a chronic inflammatory disorder of the gastrointestinal tract, and ulcerative colitis and Crohn's disease represent two major phenotypes of IBD.<sup>1,2</sup> The incidence of IBD is increasing in Europe and the United States, and the high incidence of disease recurrence is a serious healthcare problem.<sup>3,4</sup> Treatment includes anti-inflammatory drugs, immunosuppressants, and glucocorticoids to manage acute inflammation.<sup>5,6</sup> New treatment options involve inhibition of the mucosal inflammatory pathways by targeting pro-inflammatory cytokines like tumor necrosis

factor  $\alpha$  (TNF- $\alpha$ ) or cell surface receptors.<sup>7</sup> Despite treatment, 30% of patients eventually require extensive surgery on their inflamed gastrointestinal tracts because of severe inflammation, intestinal stenosis, or toxic megacolon.<sup>2,8,9</sup> Although the precise etiology and pathogenesis of IBD are not fully understood, several factors are thought to be involved in this complex disease. These factors include oxidative stress disorder, innate and adaptive immune disturbances, genetic variations, and microbial and dietary environmental factors.<sup>10,11</sup>

Nucleic acid-based medicine, which includes antisense-, small interfering RNA (siRNA)-, and microRNA (miRNA)-based therapies, shows potential as a next-generation treatment for various diseases. miRNAs are small non-coding RNAs of approximately 20–25 nucleotides that, in normal physiological processes, act to post-transcriptionally regulate the expression of multiple target genes by binding to the complementary sequences in the 3' UTR.<sup>12</sup> Recent studies have shown that miRNAs may be associated with IBD because of their roles in epithelial barrier function (miR-7, miR-21, and miR-150), autophagy (miR-13a, miR-93, miR-106, and miR-142-3p), the nuclear factor  $\kappa$ B (NF- $\kappa$ B) signaling pathway (miR-126, and miR-146a), and the interleukin-23 (IL-23) and Th17 inflammation axis (miR-20, miR-23a, miR-29b, and miR-155).<sup>13–17</sup> Therefore, these miRNAs or anti-miRs have been investigated as therapeutic tools for IBD treatment. So far, *in vivo* treatments based on miRNA or siRNA have had limited success that has been achieved using mainly liposome-based delivery methods.<sup>18,19</sup> Only 5 nucleic acid agents are currently in clinical use. These include fomivirsen and Macugen, two eye disease treatment drugs; mipomersen, which is an antisense

Received 3 March 2018; accepted 10 July 2018;  
<https://doi.org/10.1016/j.omtn.2018.07.007>

**Correspondence:** Hirofumi Yamamoto, MD, PhD, Department of Molecular Pathology, Division of Health Sciences, Graduate School of Medicine, Osaka University, Yamadaoka 1-7, Suita City, Osaka, 565-0871, Japan.

**E-mail:** [hyamamoto@sahs.med.osaka-u.ac.jp](mailto:hyamamoto@sahs.med.osaka-u.ac.jp)



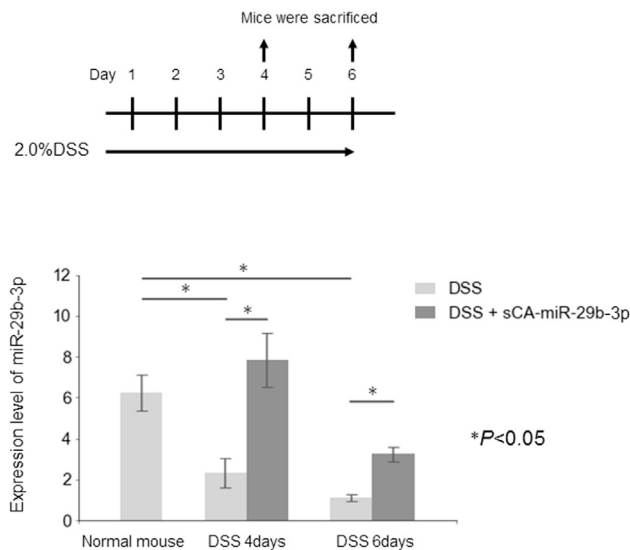


**Figure 1. miR-29b-3p Was Delivered to Inflamed Colons by sCA**

Mice were treated with 2.0% DSS for 4 or 6 days. RNA was extracted from the colons of mice. miR-29b-3p expression in the colons of DSS-treated mice decreased after DSS treatment for 4 or 6 days compared with non-DSS-treated mice. When sCA-miR-29b-3p was injected via the tail vein after DSS treatment for 4 or 6 days, miR-29b-3p levels increased significantly 4 hr after injection (\* $p < 0.05$ ,  $n = 3$  for each group).

therapeutic agent that targets apolipoprotein B100 to treat familial hypercholesterolemia; and eteplirsen, which is an antisense therapeutic agent for Duchenne muscular dystrophy.<sup>20–23</sup> Very recently, Spinraza, an antisense agent, was approved for spinal muscular atrophy. The paucity of approved RNA-based therapies reflects the fact that RNA targeting is still in the early investigational stage for most diseases.

To develop an miRNA therapy that targets IBD, this study focused on miR-29 because it has been reported that dextran sulfate sodium (DSS)-induced colitis is exacerbated in miR-29a or miR-29b knockout mice.<sup>24</sup> It is well documented that the miR-29 miRNA family (i.e., miR-29a–miR-29c) in humans targets genes that are involved in immunomodulation and cell senescence, differentiation, and apoptosis.<sup>25</sup> Because naked miRNAs are rapidly degraded in the bloodstream and are cleared by the liver and spleen, they need to be encapsulated so that a sufficient amount of miRNA can reach the target organs. For this purpose, we used a supercarbonate apatite (sCA)-based, *in vivo*, pH-sensitive delivery system for siRNA and miRNA.<sup>26</sup> This carrier simply consists of the inorganic ions  $\text{CO}_3^{2-}$ ,  $\text{Ca}^{2+}$ , and  $\text{PO}_4^{3-}$ . Systemic administration of sCA that incorporates siRNA or miRNA was used to deliver considerable amounts of nucleic acids to various tumors *in vivo*, and the nucleic acids had potent tumor-suppressive effects.<sup>26–31</sup>

Based on the success of these earlier *in vivo* cancer treatment experiments, here we examined whether sCA could deliver sufficient

amounts of miRNA to the inflamed colon and prevent profound intestinal inflammation in a mouse colitis model. As a result, we found that systemic delivery of sCA-miR-29a-3p or sCA-miR-29b-3p efficiently prevented DSS colitis, although modest amounts of miRNA were delivered to the inflamed colonic mucosa. RNA sequencing analysis revealed that miR-29a-3p and miR-29b-3p contributed to inhibition of the interferon-associated inflammatory cascade. While exploring why a small amount of miRNA was so effective, we found that the sCA-miRNA complex was preferentially captured by  $\text{CD11c}^+$  tissue dendritic cells in the colon and that this caused a molecular modulation that inhibited maturation toward pathogenic T cells. This feature of sCA may be particularly useful for efficient therapy of IBD, in which dendritic cells play a central role.

## RESULTS

### miR-29b-3p Was Delivered to the Inflamed Colon by sCA

Prior to experiments, we examined whether miR-29b-3p would be delivered by sCA to the inflamed colon. During treatment with 2.0% DSS on day 4 or day 6, miR-29b expression in the colons of DSS-treated mice significantly decreased compared with the control. miR-29b levels were restored and significantly increased 4 hr after injection of sCA-miR-29b via tail vein in mice treated with 2.0% DSS for 4 or 6 days ( $p < 0.05$ ; Figure 1).

### Treatment of Mice with DSS-Induced Colitis by Venous Injection of sCA-miR-29a-3p or sCA-miR-29b-3p

sCA-miRs were injected into the tail veins of mice on days 1, 2, 3, and 5 of 2.0% DSS treatment (Figure 2A). As shown in Figure 2B, DSS treatment destroyed the normal epithelial structure, and numerous inflammatory cells infiltrated the *lamina propria* of the distal colonic mucosa. Systemic administration of either sCA-miR-29a or sCA-miR-29b markedly prevented DSS-induced colitis, but naked miR-29b or sCA-NC miR did not have a preventive effect. The extent of inflammation was then quantitatively evaluated using well-known indicators of the DSS colitis model; i.e., body weight loss, shortening of the colon, and histological scores,<sup>32</sup> as described in the **Materials and Methods**. sCA-miR-29a or sCA-miR-29b treatment prevented body weight loss and shortening of the colon and significantly improved the histological scores compared with the sCA-negative control (NC)-miR group. In contrast, injection of naked miR-29b alone had no therapeutic effects (Figures 2c–2E). We also examined effect of sCA-miR-29b in a mouse therapeutic model of DSS colitis by referring to a report on rat IBD therapeutics<sup>33</sup> (Figure S1A). After treatment with 1.5% DSS, the distal colon had considerable colitis on day 7, and it became very severe on day 16 (Figures S1B and S1C). Systemic administration of sCA-miR-29b significantly restored DSS-induced colitis (Figures S1C and S1D).

### Comparative Analysis of Gene Expression after miR-29 Treatment of DSS Colitis

To examine gene expression in the entire inflamed mucosa, we performed an RNA sequencing analysis of DSS-treated and non-

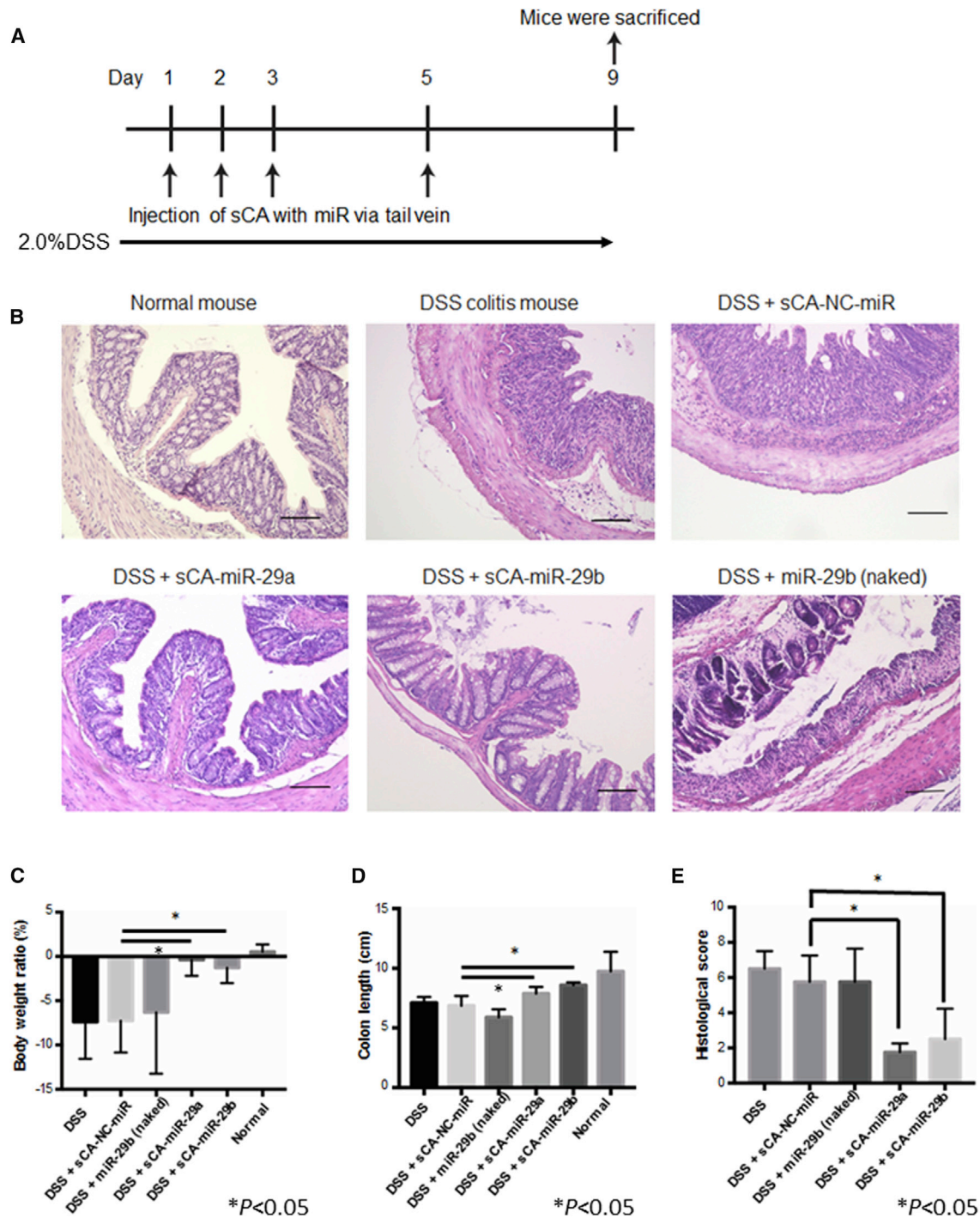


**Figure 2. Prevention of DSS-Induced Colitis by Venous Injection of sCA-miR-29a or sCA-miR-29b**

(A) The treatment schedule of DSS colitis induction and injection of sCA-miRNAs. 2.0% DSS was administered in drinking water to mice for 9 days. sCA loaded with miRNA (50  $\mu\text{g}$ ) was injected on days 1, 2, 3, and 5. The mice were divided into 6 groups of 5 mice as follows: non-DSS-treated mice, DSS-treated mice, DSS+sCA-NC-miR mice, DSS+sCA-miR-29a mice, DSS+sCA-miR-29b mice, and DSS+naked miR-29b mice. (B) Representative images of H&E-stained distal colonic mucosae. The distal colon is usually the most affected by DSS-induced colitis. In DSS+sCA-miR-29a mice and in DSS+sCA-miR-29b mice, the mucosal structures appeared almost normal with few infiltrating inflammatory cells. Scale bars, 100  $\mu\text{m}$ . (C) Changes in body weight. The change in body weight was significantly lower in DSS+sCA-miR-29a and DSS+sCA-miR-29b mice than in the DSS+sCA-NC-miR group (\* $p < 0.05$ ). (D) Compared with DSS+sCA-NC-miR mice, the colorectal tract was significantly longer in both DSS+sCA-miR-29a and DSS+sCA-miR-29b mice (\* $p < 0.05$ ). (E) The histological score was significantly lower in DSS+sCA-miR-29a and DSS+sCA-miR-29b mice than in DSS+sCA-NC-miR mice (\* $p < 0.05$ ).

(legend continued on next page)

DSS-treated colon walls (Figure S2A; Table S2). By comparing the expression levels of mRNAs in DSS-treated, NC-miR-treated mice on day 4 with DSS-untreated mice (Figure S2B, lane 3 versus lane 1), we identified genes that showed enhanced expression (>2.0-fold,  $p < 0.05$ ) or reduced expression (<0.5-fold,  $p < 0.05$ ) in DSS-treated mice. A tendency for the genes to be upregulated or downregulated was also noted in the DSS-treated, NC-miR-treated group on day 2 compared with DSS-untreated mice (Figure S2B, lane 2 versus lane 1). Heatmap analyses suggested that the expression of several genes involved in the type I or type II interferon pathways (e.g., Stat1, Stat2, IRF7, IRF9, and IFIT1) was upregulated on day 4 of DSS treatment in the NC-miR group compared with normal control samples (Figure S3). Gene ontology (GO) analysis indicated that the interferon signaling pathway emerged first among the activated signaling pathways of DSS treatment in the NC-miR group on day 4 (Figure S4A). Ingenuity Pathway Analysis indicated that many proteins, including those in the interferon signaling pathway, were theoretically activated based on the gene expression profile on day 4 of DSS treatment in the NC-miR group (Figures 3A–3C; Figure S4B). This activation was partly inhibited individually or in combination by administration of sCA-miR-29a or sCA-miR-29b (Figure 3A).

#### Subcutaneous Injection of sCA-miR-29b

We also examined the efficacy of sCA-miR-29b when it was administered through a subcutaneous injection. Subcutaneous injection of sCA-miR-29b had a marked preventive effect on DSS-induced colitis on day 9 (Figures 4A–4E).

#### Co-localization of miR-29b with CD11c<sup>+</sup> Dendritic Cells in Colonic Mucosa

To visualize the extent and localization of miR-29b in the inflamed colon, we used Alexa Fluor 647-conjugated miR-29b. Thus, after 2.0% DSS treatment for 7 days, sCA incorporating miR-29b tagged with Alexa Fluor 647 was administered subcutaneously, and mouse colons were excised 4 hr after administration. Fluorescence microscopy showed that the red fluorescence of Alexa Fluor 647-conjugated miR-29b was present in the mucosa and submucosa of the colonic epithelium, but it was, unexpectedly, rather scarce (Figure S5) for the drastic preventive effect of DSS-induced colitis by miR-29b.

To further investigate the localization of miR-29b in relation to immune cells, we performed immunostaining for various immune cell types. These include Gr-1 (Ly-6G) for neutrophils, F4/80 for macrophages, CD4 for helper T cells, CD8 for killer T cells, B220 (CD45R) for B cells, and CD11c for dendritic cells (Figure 5A; Figure S6). It was revealed that miR-29b mostly co-localized with CD11c<sup>+</sup> dendritic cells and occasionally co-localized with B220 (CD45R)<sup>+</sup> B cells but not with other immune cells. RT-PCR for miR-29b levels in CD11c<sup>+</sup> cells and CD11c<sup>-</sup> cells that were isolated using the AutoMACS Pro separator indicated that miR-29b was preferentially accumulated in CD11c<sup>+</sup> dendritic cells (DCs) 4 hr after injection ( $p < 0.05$ ; Figure 5B).

To further investigate the mechanisms underlying the effects of the miR-29b taken up in CD11c<sup>+</sup> DCs, we collected DCs from the inflamed colon and examined critical gene expression by RT-PCR as described previously.<sup>34</sup> DCs play a key role in the initial stage of the inflammatory immune reaction in DSS-induced colitis.<sup>35,36</sup> It has been demonstrated that miR-29a and miR-29b knockout mice had an increased level of IL-23 in DCs,<sup>24</sup> which is one of the major molecules for IBD formation. The cytokines IL-6 and TGF- $\beta$  are also important because they drive naive T cells to become Th17 intestinal immune T cells.<sup>37</sup> qRT-PCR showed that treatment with sCA-miR-29a or sCA-miR-29b significantly decreased the levels of the IL-23 subunits IL-12p40 and IL-23p19, respectively, in DCs from DSS-treated mouse colons (Figure 5C). Injection of sCA-miR-29a and sCA-miR-29b also significantly decreased IL-6 and TGF- $\beta$  mRNA expression in CD11c<sup>+</sup> DCs; notably, these are otherwise upregulated by DSS treatment (Figure 5C).

#### sCA Efficiently Delivers miRNA into CD11c<sup>+</sup> DCs in the Lamina Propria of the Colonic Mucosa

We attempted to examine whether this targeting of CD11c<sup>+</sup> DCs by sCA-miR-29b was specific to miR-29b or because of an unspecific feature of sCA irrespective of miRNA species. For this purpose, we used an NC miRNA tagged with Alexa Fluor 647 for histological analysis and a non-natural (artificial) miRNA for qRT-PCR that is not naturally found in mice (Table S1). DSS-treated mice had a significantly higher level of the artificial miRNA than non-DSS-treated mice at all sites of the colon and ileum ( $p < 0.05$ ; Figure 6A). Microscopy showed only a few red fluorescence spots corresponding to the Alexa Fluor 647-tagged NC-miR in the normal colonic mucosa and in the DSS-treated inflamed colonic mucosa, and the latter had more red spots in the lamina propria of the mucosa (Figure 6B).

Fluorescence microscopy showed that the red signals of subcutaneously injected artificial miRNAs very often overlapped with the green signals of CD11c<sup>+</sup> DCs in the DSS-treated colonic mucosa (Figure 7A). qRT-PCR analyses confirmed that the subcutaneously administered exogenous miRNA was detected at high levels in CD11c<sup>+</sup> DCs compared with CD11c<sup>-</sup> cells in the DSS-treated inflamed mucosa ( $p < 0.05$ ; Figure 7B). Confocal microscopy showed that the CD11c<sup>+</sup> green signals were on the cell surfaces of DCs, whereas the miRNA red signals were found in the cytoplasm (Figure 7C).

#### Local Administration of sCA-miR-29b

Finally, we examined the efficacy of sCA-miR-29b when it was administered via the *trans*-anal route (enema). In contrast to systemic administration, *trans*-anal delivery of an sCA-miR-29b solution to the rectum and colon had no inhibitory effects on DSS-induced colitis (Figures 8A–8F).

#### DISCUSSION

In 2008, systemic delivery of cyclin D1 siRNA via venous injection was reported in DSS-induced colitis using liposomes.<sup>38</sup> However,





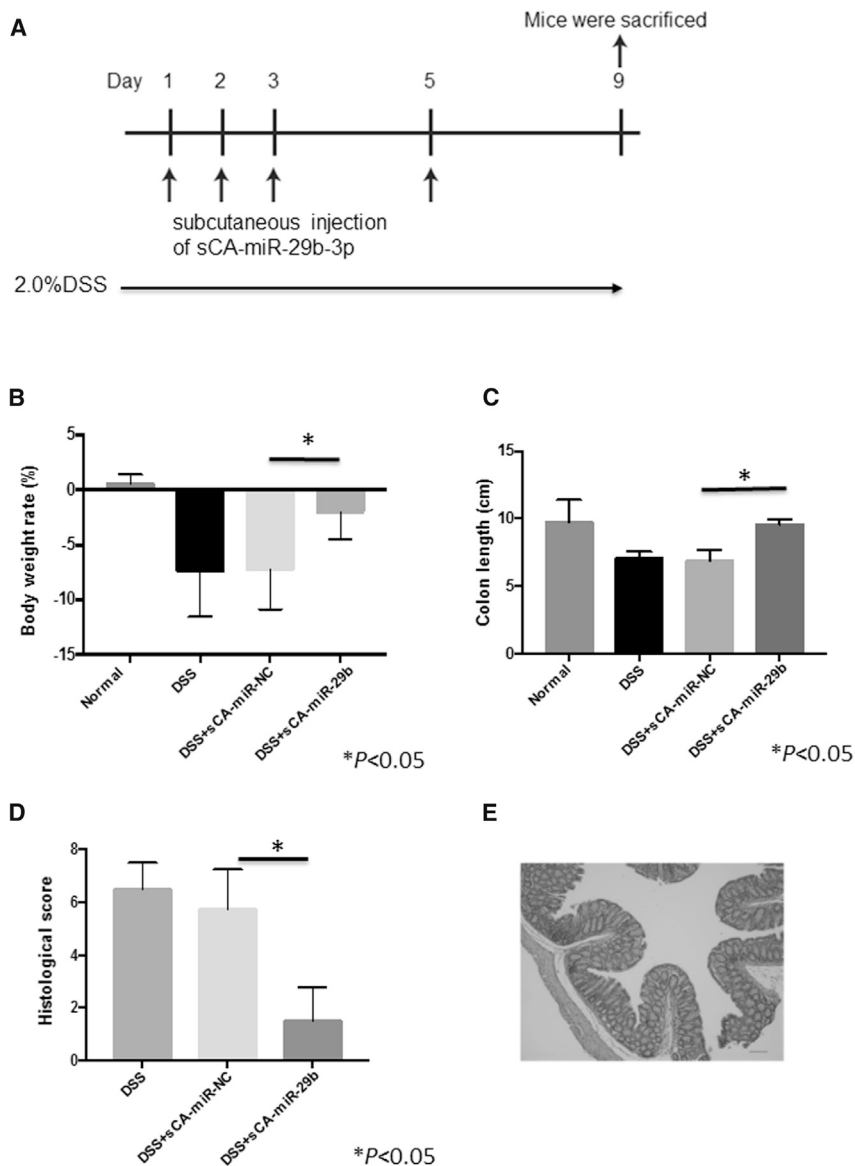


**Figure 4. Effects of Subcutaneous Injection of sCA-miR-29b in the DSS Colitis Mouse Model**

(A) After we began giving 2.0% DSS to mice in their drinking water for 9 days, sCA+miR-29b (50  $\mu$ g) or sCA+NC-miR was administered by subcutaneous injection on days 1, 2, 3, and 5 ( $n = 5$  for each). Mice were sacrificed on day 9. (B–D) Compared with DSS treatment alone or treatment with DSS+sCA-NC-miR, (B) body weight loss, (C) colon shortening, and (D) histological scores are shown. (E) Histological changes in mice treated with DSS+sCA-miR-29b were better. Scale bar, 100  $\mu$ m.

tein (PTBP) as well as miR-340, miR-4689, miR-302, miR-369, and miR-29b-1-5p more efficiently than conventional *in vivo* delivery systems.<sup>26–31</sup> The sCA-nucleic acid complexes were found in the intracellular compartments of subcutaneous tumors as early as 90 min after injection and achieved rapid endosomal escape, and RNA function was fully realized in every case. Basically, the potent anti-tumor effects were based on massive transport of nucleic acids into the cytoplasm of tumor cells. Unexpectedly, in this IBD model, we found that miRNA delivery to the inflamed colon was much less efficient than we had anticipated. Therefore, we were very surprised to find that sCA-miR-29a and sCA-miR-29b efficiently prevented inflammation associated with DSS-induced colitis with such minimal amounts of miRNA. When we injected the naked miR-29b alone or the sCA-NC-miR, no therapeutic effects were obtained, suggesting that the naked miRNA underwent rapid degradation in the bloodstream and that sCA played an essential role in optimizing the effects of miR-29a and miR-29b. In the therapeutic model, we modified the protocol of the therapeutics of rat DSS colitis<sup>34</sup> and administered 1.5% DSS for 16 days instead of 2.0%

systemic administration of siRNA remains a clinical challenge. Therefore, subsequent studies mainly investigated oral or enteral administration of nucleic acids using polysaccharide-based nanoparticles, polylactide (PLA)-based nanoparticles, the nanoparticles-in-microsphere oral system (NiMOS), thioketal-based nanoparticles, or polyethyleneimine (PEI)-based nanoparticles as carriers.<sup>39–41</sup> SMAD7 antisense oligonucleotide may move up to the clinical stage as an oral agent against Crohn's disease.<sup>42</sup> However, there are no reports of therapeutic success using systemic delivery of miRNA in an IBD model.

In our previous tumor treatment studies, we found that sCA nanoparticles represent an innovative delivery system that could be used to deliver siRNA for survivin and polyprimidine tract-binding pro-

DSS for 7–9 days, which was used in the prevention model. As a result, we found that sCA-miR-29b was able to restore DSS colitis when treatment started on day 5 (Figure S1). In contrast, when we administered sCA-miR-29b by *trans*-anal instillation (i.e., via enema), DSS colitis showed no improvement. This could be attributable to the acidic colonic lumen (pH 2.3–5.5) in IBD intestinal tracts,<sup>39</sup> where sCA readily undergoes degradation because of its pH-sensitive structure.

Although miR-29b and NC-miRNA delivered by sCA were small in the inflamed colon, we found that they were often captured by CD11c<sup>+</sup> DCs. Analysis of CD11c<sup>+</sup> DCs revealed that the sCA-miR-29a and sCA-miR-29b treatment groups showed decreases in the IL-23 subunits IL-12p40 and IL-23p19, respectively. These findings

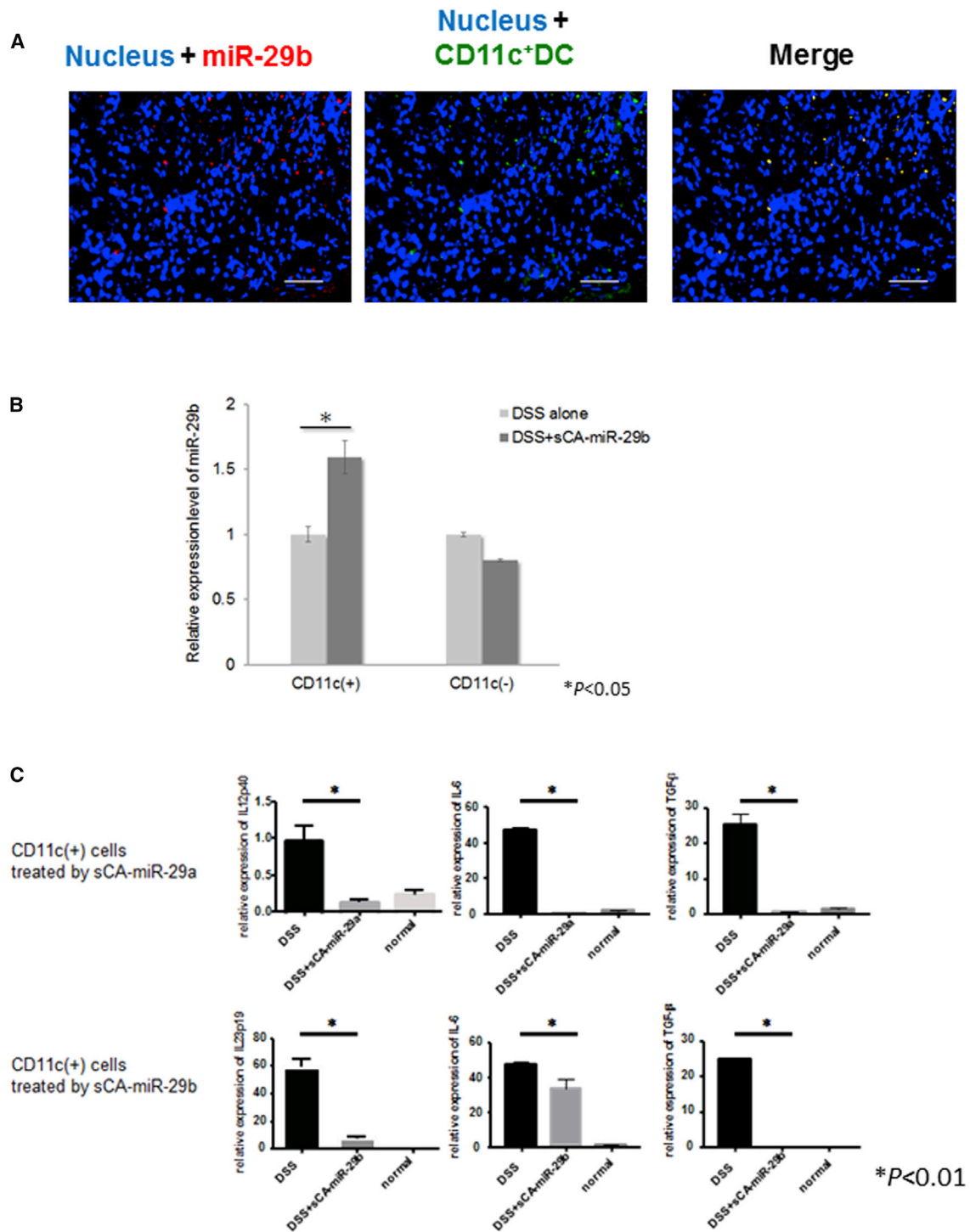
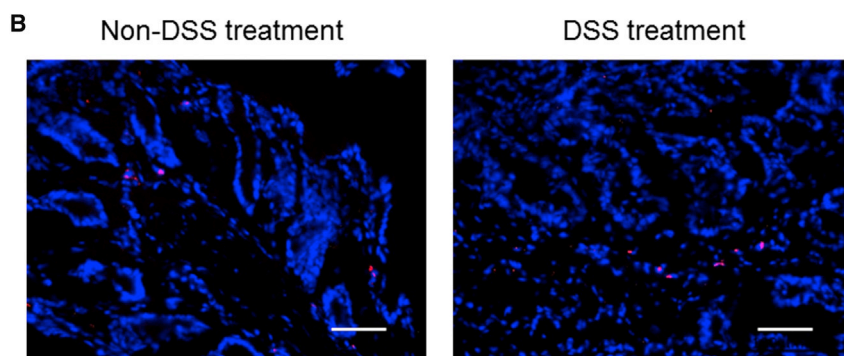
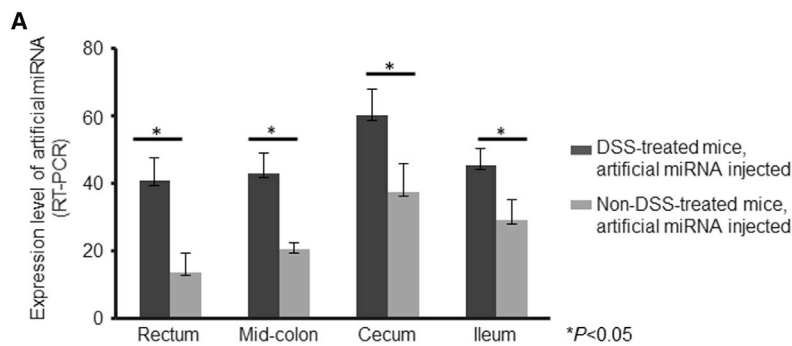


**Figure 5. Alexa Fluor 647-Tagged miR-29b Was Efficiently Incorporated into CD11c<sup>+</sup> Dendritic Cells in a DSS-Induced Colitis Mouse Model**

(A) Distribution of Alexa Fluor 647-conjugated miR-29b and CD11c<sup>+</sup> DCs. Fluorescence microscopy showed that miR-29b miRNAs (red signals) mostly co-localized with CD11c<sup>+</sup> DCs (green signals). Scale bars, 50  $\mu$ m. (B) *Lamina propria* cells were collected from the mucosa after gentle enzymatic digestion, and CD11c<sup>+</sup> cells and CD11c<sup>-</sup> cells were isolated using the AutoMACS Pro separator. Exogenously administered miR-29b was preferentially accumulated in CD11c<sup>+</sup> DCs (\* $p$  < 0.05). (C) After we began giving 2.0% DSS to mice in their drinking water, sCA-miR-29a and sCA-miR-29b were intravenously administered on days 1, 2, and 3, and the colons were removed on day 4. CD11c<sup>+</sup> cells were isolated using the AutoMACS Pro separator. qRT-PCR analysis indicated that sCA-miR-29a suppressed the expression of IL-12 p40, IL-6, and TGF- $\beta$ , whereas sCA-miR-29b significantly inhibited the expression of IL-23p19, IL-6, and TGF- $\beta$  (\* $p$  < 0.01,  $n$  = 3 mice in each group).



Red spots: Alexa Fluor 647 conjugated NC miRNA

are consistent with a report by Becker et al.<sup>35</sup> that IL-23 production was mediated by DCs. It has also been reported that IL-12p40 is a direct target of miR-29a and that IL-23p19 is an indirect target of miR-29b.<sup>24</sup> Moreover, sCA-miR-29a and sCA-miR-29b also inhibited the expression of IL-6 and TGF- $\beta$  mRNA in DCs; both of these are important for the differentiation of naive T cells into Th17 cells, which are one type of intestinal immune T cells involved in the development of IBD.<sup>35–37,43</sup> Based on these findings, we raise the following hypothesis. DCs in the *lamina propria* of the damaged mucosa capture bacteria and food fragments and present certain antigens that drive naive T cells to become effector (differentiated) T cells. The DCs also secrete IL-23, which activates Th-17 cells; these become pathogenic Th-17 cells.<sup>44</sup> miR-29s inhibit the differentiation of naive T cells into Th-17 cells by downregulating IL-6 and TGF- $\beta$  and by preventing the conversion of Th17 cells into pathogenic Th17 cells by suppressing the IL-23 subunits IL-12p40 and IL-23p19 (Figure S7).

The SMAD7 antisense oligonucleotide, which should activate the TGF- $\beta$  signaling pathway is a useful oral agent against Crohn's disease.<sup>42</sup> Because we showed that miR-29s rather suppressed TGF- $\beta$  expression as well as IL-6 and IL-23, this may be the next challenge when developing the ideal IBD therapy. Combination therapy of miR-29s and other miRNAs that enhance the TGF- $\beta$  signaling pathway may be an option.

#### Figure 6. Distribution of Exogenous miRNA in Non-DSS-Treated Mice and in DSS-Treated Mice

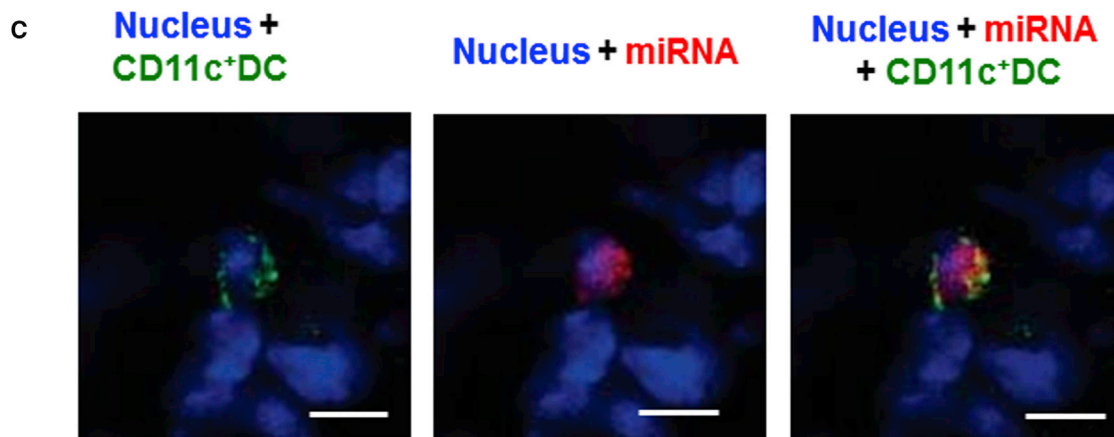
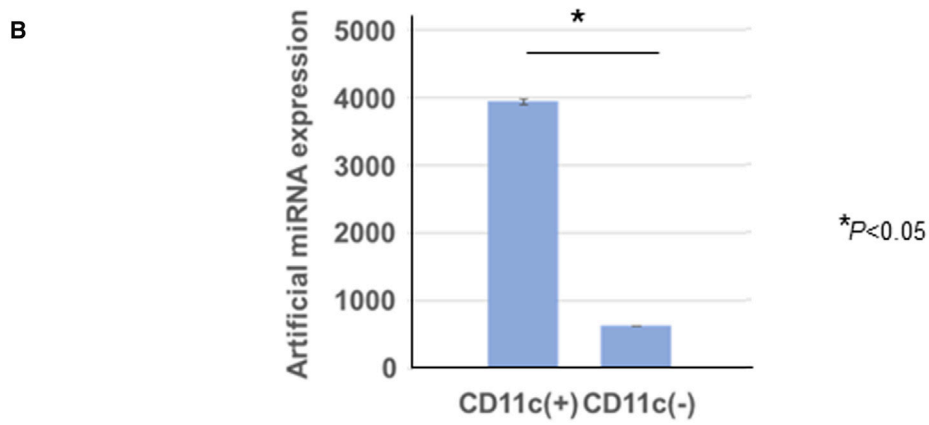
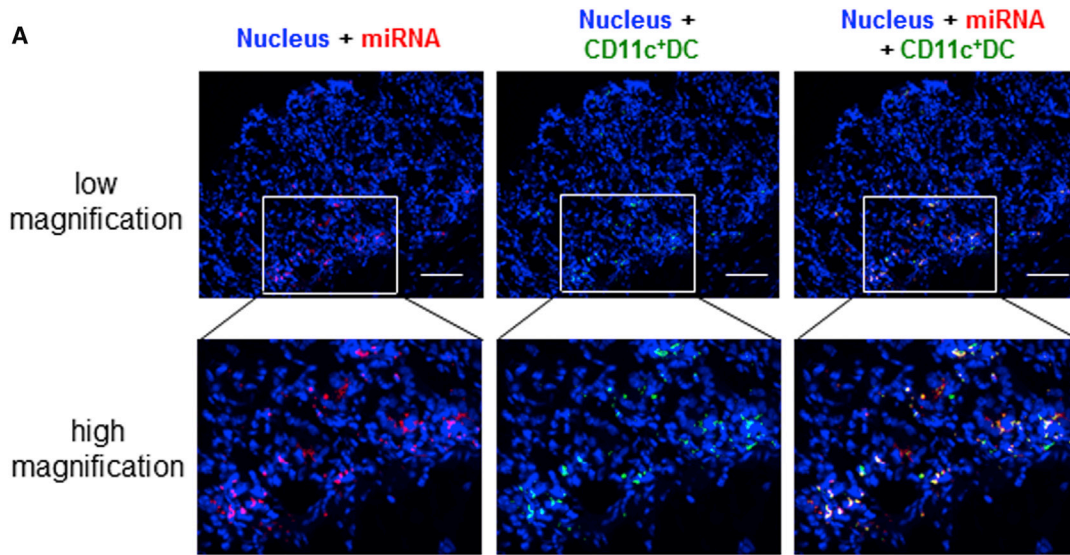
(A) After 2.0% DSS in drinking water was given to the mice for 7 days, sCA incorporating a non-natural artificial miRNA (50  $\mu$ g; sequence in Table S1) was injected into the tail vein. The level of this miRNA was significantly higher in DSS-treated mice than in non-DSS-treated mice at each site ( $*p < 0.05$ ,  $n = 3$  for each group). (B) Localization of the negative control (NC) miRNA, which was tagged with Alexa Fluor 647, in colonic mucosae. After 2.0% DSS in drinking water was given to the mice for 7 days, sCA incorporating an NC miRNA tagged with Alexa Fluor 647 (50  $\mu$ g) was injected into the tail vein. Colon samples were excised 4 hr later. Fluorescence microscopy showed little red fluorescence (Alexa Fluor 647) in non-DSS-treated colonic epithelia, whereas the red signal was greater, although not strong, in the epithelia of DSS-treated colon samples. Scale bars, 100  $\mu$ m.

RNA sequencing analysis of the colon walls suggested that DSS treatment activated interferon signaling pathways, which ranked at the top position in gene ontology analysis and in fifth position by Ingenuity Pathway Analysis (Figures S4A and S4B). Ingenuity Pathway Analysis further showed that miR-29a and miR-29b, individually or in combination, could reverse the effects of DSS on highly activated molecules associated with the interferon signaling pathways (Figure 3). These findings suggest that blocking the initial immune reaction in DCs by miR-29s may suppress the subsequent spread of the inflammatory cascade.

We are not certain at present how the sCA-miRNA complex preferentially accumulates at CD11c<sup>+</sup> DCs. Specifically, subcutaneously injected sCA-miR-29b was found mostly in CD11c<sup>+</sup> DCs by microscopy and by RT-PCR after cell sorting. This was associated with marked inhibition of colitis. Because not only miR-29b but also NC-miR accumulated in CD11c<sup>+</sup> DCs, this might be due to the phagocytosis action of DCs. We also found that miR-29b was occasionally incorporated by B220 (CD45R)<sup>+</sup> B cells, but no correlation was found in tissue distribution between miR-29b and other immune cell types, including T cells, macrophages, and neutrophils. The red fluorescence of Alexa Fluor 647-conjugated miR-29b was rather scarce in the colonic epithelium.

One may speculate where the remaining sCA-miRNA goes after injection into mice. In our recent study, we reported that indocyanine green (ICG) loaded on sCA was distributed largely in the liver and kidney in addition to tumors.<sup>45</sup> When we examined the distribution of the artificial miRNA by RT-PCR after injection of the sCA-miRNA complex into the tail vein, we found that the artificial miRNA was mainly distributed in the liver, followed by the spleen to some extent (Figure S8). Compared with these organs, sCA-miRNA uptake in the





(legend on next page)

colon and intestine was only minimal. We also found that DSS treatment did not enhance miRNA uptake in normal organs, but, rather, that it decreased miRNA uptake in the spleen and lung.

Viral vectors, including retroviruses and adeno-associated viruses, have been used to introduce gene expression in target organs in animal models because of their high transfection efficiency. However, the potential side effects of genomic integration into the host genome have limited the clinical applications of these vectors. For example, long-term use of gene therapy for X-linked severe combined immunodeficiency (SCID-X1) leads to acute leukemia.<sup>46</sup> Non-viral nanoparticles are safer and, thus, preferable as a delivery method. However, it is emphasized that RNAi-based nanosystems must be improved substantially for use of siRNA or miRNA as IBD therapy.<sup>39</sup> In this context, the present data demonstrating the *in vivo* effectiveness of the sCA-miR-29a or sCA-miR-29b complexes show that this system is promising in terms of clinical potential. Our previous study showed that repeated administration or 5-fold greater amounts of sCA alone did not cause toxicity in mice.<sup>26</sup> Moreover, our recent studies showed that ICG<sup>45</sup> or miRNA<sup>31</sup> loaded on sCA efficiently accumulated in tumors and that it did not cause any abnormalities in blood chemistry tests or histology of normal organs of mice. However, considerable uptake of miRNA or ICG loaded on sCA in the liver (Figure S8; Tamai et al.<sup>45</sup>) may cause clinical problems, as is the case with many viral and non-viral vehicles. To overcome this issue, development of an improved vehicle for clinical use is currently underway in our laboratory.

We and other investigators have shown that miR-29b is a potent tumor suppressor and a prognostic factor for various human malignancies, including colorectal cancer, lung cancer, lymphoma, and acute myeloid leukemia, because it regulates cell cycle progression and apoptosis.<sup>47–52</sup> These findings suggest that miR-29b may be a promising next-generation treatment for cancer. As for IBD, it is known that IL-23 levels increase in patients with Crohn's disease.<sup>24,33</sup> On the other hand, several studies showed that miR-29a and miR-29b levels are elevated in patients with chronic IBD,<sup>14,53</sup> which might be a feedback reaction to suppress IL-23. It has also been demonstrated that there is significant downregulation of miR-29b in mucosae overlying strictures in Crohn's disease patients compared with paired mucosae overlying non-strictured areas.<sup>54</sup> This suggests that a severe disease status may be linked to a decrease in miR-29b expression. Taken together, detailed analysis of human IBD samples in relation to disease severity may be essential prior to clinical application.

In conclusion, our data show that systemically administered sCA-miR was often found in CD11c<sup>+</sup> DCs in the inflamed colon and that sCA-miR-29a or sCA-miR-29b prevented DSS colitis by suppressing interferon-related cascades. The present study suggests the possibility that sCA-miR-29s may be useful for IBD therapy.

## MATERIALS AND METHODS

### Animals

Seven-week-old BALB/c mice, which have an intact immune system, were purchased from CLEA (Tokyo, Japan). The animal experiments in this study were approved by the Institutional Animal Care and Use Committee of Osaka University Graduate School of Medicine and by the Committee for the Ethics of Animal Experiments of Osaka University (permit 260033-006). Surgery was performed under sodium pentobarbital anesthesia, and every effort was made to minimize suffering. To generate experimental colitis, DSS (36,000–50,000 molecular weight [MW]; MP Biomedicals, Santa Ana, CA) was given to BALB/c mice in their drinking water at a concentration of 2.0% for 7 to 9 days. In the therapeutic models, 1.5% DSS was administered to BALB/c mice for 16 days.

### Histological Inflammation Scoring of DSS-Induced Colitis

The extent of colonic and intestinal wall inflammation was scored as reported previously.<sup>32</sup> Mucosal damage: 0, normal; 1, focal damage plus 3–10 intraepithelial lymphocytes (IELs)/high power field (HPF); 2, rare crypt abscesses plus more than 10 IELs/HPF; 3, multiple crypt abscesses and erosion or ulceration plus more than 10 IELs/HPF. Submucosal damage: 0, normal or widely scattered leukocytes; 1, focal aggregates of leukocytes; 2, diffuse leukocyte infiltration with expansion of the submucosa; 3, diffuse leukocyte infiltration. *Muscularis* damage: 0, normal or widely scattered leukocytes; 1, widely scattered leukocyte aggregates between muscle layers; 2, leukocyte infiltration with focal effacement of the *muscularis*; 3, extensive leukocyte infiltration with transmural effacement of the *muscularis*.

### miRNAs

The specific miRNAs (mmu miR-29a-3p, mmu miR-29b-3p) and the negative control miRNA used in the *in vivo* analysis were purchased from Gene Design (Osaka, Japan). Alexa Fluor 647 fluorescent dye (red signal) was conjugated to the NC miRNA or miR-29b-3p with a junk sequence to visualize the miRNA distribution in the tissue samples. To measure exogenous miRNA in the tissue by RT-PCR, non-natural miRNA was synthesized; this miRNA was 62.5% identical to mmu miR-29b-3p, which is not

## Figure 7. sCA Efficiently Delivers NC miRNA into CD11c<sup>+</sup> DCs in the Lamina Propria of the Colonic Mucosa

(A) After 2.0% DSS was given to mice in their drinking water for 7 days, sCA incorporating the NC miRNA tagged with Alexa Fluor 647 was administered subcutaneously, and mouse colons were excised 4 hr after administration. Fluorescence microscopy showed that NC miRNAs (red signals) mostly co-localized with CD11c<sup>+</sup> DCs (green signals). Scale bars, 100  $\mu$ m. (B) *Lamina propria* cells were collected from the mucosa after gentle enzymatic digestion, and CD11c<sup>+</sup> cells and CD11c<sup>-</sup> cells were isolated using the AutoMACS Pro separator. The miRNA level was significantly higher in CD11c<sup>+</sup> DCs than in CD11c<sup>-</sup> cells (\**p* < 0.01). Mice that were not injected with miRNA gave no measurable values (data not shown). (C) Confocal microscopy of a single dendritic cell in a mouse with DSS-induced colitis. CD11c<sup>+</sup> green signals are on the cell surface, whereas red miRNA signals are in the cytoplasm. The nuclei are blue (DAPI). Scale bars, 5  $\mu$ m.

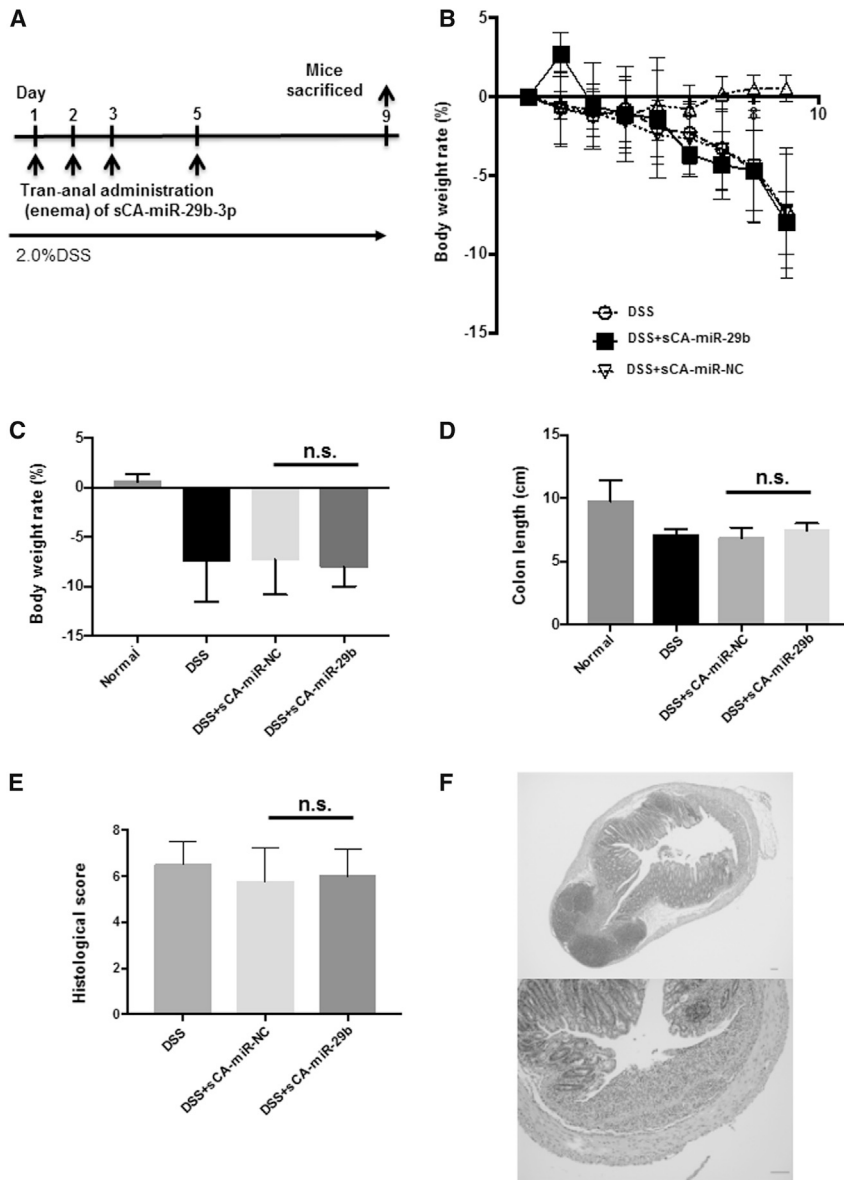


**Figure 8. The Effects of *trans*-Anal Administration (Enema) of sCA+miR-29b in DSS Colitis Mice**

(A) 2.0% DSS in drinking water was given to the mice for 7 days, and sCA+miR-29b (50  $\mu$ g) or sCA+NC-miR was administered via the *trans*-anal route on days 1, 2, 3, and 5 ( $n = 5$  for each). Mice were sacrificed on day 9. (B–F) Compared with sCA-NC-miR mice and DSS treatment-only mice, there were no significant changes in body weight (B and C), colon length (D), histological score (E), or histological change (F) in sCA+miR-29b-treated mice. Scale bars, 100  $\mu$ m.

FITC-conjugated goat anti-rat immunoglobulin G (IgG) was used (Jackson ImmunoResearch Laboratories, West Grove, PA). The nuclei were stained with ProLong Gold anti-fade reagent with DAPI (Invitrogen, Carlsbad, CA). Sections were observed using a fluorescence microscope (BZ-X 700, Keyence, Osaka, Japan).

#### Production of sCA

sCA was prepared as described previously.<sup>26</sup> Briefly, miRNA (100  $\mu$ g) was incubated in 50 mL of inorganic solution (44 mM NaHCO<sub>3</sub>, 0.9 mM NaH<sub>2</sub>PO<sub>4</sub>, and 1.8 mM CaCl<sub>2</sub> [pH 7.5]) at 37°C for 30 min. The solution was centrifuged at 12,000 rpm for 3 min, and the pellet containing miRNA was dissolved in saline containing 0.5% albumin. This solution was sonicated (38 kHz, 80 W) in a water bath for 10 min. Each injection contained 50  $\mu$ g of miRNA dissolved in 200  $\mu$ L of physiological saline.

#### mRNA and miRNA Expression

Total RNA and miRNA were extracted from tissue samples using the miRNeasy kit (QIAGEN, Hilden, Germany). RNA quality was assessed with a NanoDrop ND-1000 spectrophotometer (NanoDrop Technologies, Rockland, DE), and

2  $\mu$ g of RNA was reverse-transcribed with the High-Capacity RNA to cDNA Kit (Applied Biosystems, Foster City, CA). The resulting cDNA was amplified using the following specific primers:

IL-6 forward, 5'-AGTTGCCTTCTGGGACTGA-3'; IL-6 reverse, 5'-CAGAATTGCCATTGCACAAC-3'

TGF- $\beta$  forward, 5'-TTGCTTCAGCTCCACAGAGA-3'; TGF- $\beta$  reverse, 5'-TGGTTGTAGAGGGCAAGGAC-3'

IL-12p40 forward, 5'-AGGTGCGTTCCTCGTAGAGA-3'; IL-12p40 reverse, 5'-AAAGCCAACCAAGCAGAAGA-3'

IL-23p19 forward, 5'-GACTCAGCCAACCTCCTCCAG-3'; IL-23p19 reverse, 5'-GGCACTAAGGGCTCAGTCAG-3'

found in mice. The miRNAs used in this study are shown in Table S1.

#### Immunofluorescence

Specimens were frozen in optimal cutting temperature (OCT) compound, and 8- $\mu$ m sections were cut and fixed in 4% paraformaldehyde. The frozen sections were incubated overnight with the following antibodies: Fluorescein (FITC)-conjugated mouse CD11c antibody (BioLegend, San Diego, CA), rat anti-mouse Ly-6G or Ly-6C (Gr-1) antibody (BioLegend), rat anti-mouse CD4 antibody (BD Biosciences, San Jose, CA), Alexa Fluor 488-conjugated rat anti-mouse CD8a antibody (BioLegend), rat anti-mouse F4/80 antibody (Bio-Rad, Hercules, CA), and rat anti-mouse CD45R (Bio-Rad) at a concentration of 1:100. As a secondary antibody,

qRT-PCR of mRNA was performed with the LightCycler 480 real-time PCR system (Roche Diagnostics, Basel, Switzerland). Amplification data were normalized to  $\beta$ -actin expression. qRT-PCR of miRNA was performed with the ABI Prism 7900HT sequence detection system using TaqMan miRNA assays for hsa-miR-29a (ID 002112), hsa-miR-29b (ID 000413), RNU6B (ID 001093), and miR-29b derivative miRNA (ID CSBJWVW). Amplification data were normalized to endogenous RNU6B expression, and relative expression was quantified using the  $2^{-DDCt}$  method.

#### Isolation of CD11c<sup>+</sup> DCs from the Lamina Propria of the Colonic Mucosa

Colonic DCs were collected as described previously.<sup>34</sup> Briefly, the intestinal mucosa was washed in PBS to remove feces, placed in Hank's balanced salt solution (HBSS) containing 5 mM EDTA, and incubated for 20 min with shaking. The tissue was cut into small pieces that were incubated in RPMI 1640 medium containing 4% fetal bovine serum (FBS), 1 mg/mL collagenase D (Roche Life Science, Mannheim, Germany), 0.5 mg/mL dispase (Invitrogen, Carlsbad, CA), and 50  $\mu$ g/mL DNase I (Roche Life Science) for 50 min in a 37°C shaking water bath. Digested tissues were then resuspended in HBSS containing 5 mM EDTA and passed through a 40- $\mu$ m cell strainer. Anti-CD11c MicroBeads (100  $\mu$ L; Miltenyi Biotec, Bergisch Gladbach, Germany) were mixed with the cell pellet after it was resuspended in 500  $\mu$ L buffer. The cell and microbead mixture was incubated for 15 min at 4°C, and then the cells were processed using the AutoMACS Pro separator (Miltenyi Biotec) according to the manufacturer's protocol.

#### RNA Sequencing

Library preparation was performed using a TruSeq stranded mRNA sample prep kit (Illumina, San Diego, CA) according to the manufacturer's instructions. Sequencing was performed on an Illumina HiSeq 2500 platform in 75-base single-end mode. Illumina Casava1.8.2 software was used for base calling. The sequenced reads were mapped to the mouse reference genome sequences (mm10) using TopHat version 2.0.13 in combination with Bowtie2 version 2.2.3 and SAMtools version 0.1.19. The fragments per kilobase of exon per million mapped fragments (FPKM) were calculated using Cuffnorm version 2.2.1. A series of enhanced (>2.0-fold,  $p < 0.05$ ) or reduced (<0.5-fold,  $p < 0.05$ ) genes were identified for further gene expression analysis. The raw data were deposited in the NCBI GEO database under accession number GSE93162. The processes and upstream regulators were identified using QIAGEN's Ingenuity Pathway Analysis (IPA, QIAGEN, Redwood City; <https://www.qiagen.com/ingenuity>) using default settings.

#### Statistics

The statistical significance of differences between 2 groups was calculated by Student's *t* test. When more than 2 groups were compared, one-way ANOVA was used, followed by Holm-Sidak's multiple comparisons test to determine the statistical significance of the differences. Statistical analyses were performed using the JMP12 program (SAS Institute, Cary, NC) and GraphPad Prism version 7.00 for Mac

(GraphPad, San Diego, CA). Differences with  $p < 0.05$  were considered to be significant.

#### SUPPLEMENTAL INFORMATION

Supplemental Information includes seven figures and two tables and can be found with this article online at <https://doi.org/10.1016/j.omtn.2018.07.007>.

#### AUTHOR CONTRIBUTIONS

T.F., D.O., H.H., Y.K., K.N., and N.T. conducted the experiments. T.M., J.N., H.K., K.T., X.W., and A.I. performed specific techniques for immunology or drug delivery. N.M., N.H., H.T., T.H., C.M., Y.D., and M.M. interpreted of each result and proposed the appropriate next steps. H.Y. designed the experiments. T.F., Y.Y., and H.Y. wrote the paper.

#### CONFLICTS OF INTEREST

The authors declare no conflicts of interest.

#### ACKNOWLEDGMENTS

This study was supported by the Japan Society for The Promotion of Science, JSPS KAKENHI Grant-in-Aid for Challenging Exploratory Research JP 16K15590, and a research grant from The Osaka Medical Research Foundation for Intractable Diseases to H.Y.

#### REFERENCES

- Bouma, G., and Strober, W. (2003). The immunological and genetic basis of inflammatory bowel disease. *Nat. Rev. Immunol.* 3, 521–533.
- Fiocchi, C. (1998). Inflammatory bowel disease: etiology and pathogenesis. *Gastroenterology* 115, 182–205.
- Benchimol, E.I., Fortinsky, K.J., Gozdyra, P., Van den Heuvel, M., Van Limbergen, J., and Griffiths, A.M. (2011). Epidemiology of pediatric inflammatory bowel disease: a systematic review of international trends. *Inflamm. Bowel Dis.* 17, 423–439.
- Sasaki, H., Ikeuchi, H., Bando, T., Hirose, K., Hirata, A., Chohn, T., Horio, Y., Tomita, N., Hirota, S., Ide, Y., et al. (2017). Clinicopathological characteristics of cancer associated with Crohn's disease. *Surg. Today* 47, 35–41.
- Kimura, H., Takahashi, K., Futami, K., Ikeuchi, H., Tatsumi, K., Watanabe, K., Maeda, K., Watadani, Y., Nezu, R., Kameyama, H., et al. (2016). Has widespread use of biologic and immunosuppressant therapy for ulcerative colitis affected surgical trends? Results of a questionnaire survey of surgical institutions in Japan. *Surg. Today* 46, 930–938.
- Irvine, E.J., Feagan, B., Rochon, J., Archambault, A., Fedorak, R.N., Groll, A., Kinnear, D., Saibil, F., and McDonald, J.W.; Canadian Crohn's Relapse Prevention Trial Study Group (1994). Quality of life: a valid and reliable measure of therapeutic efficacy in the treatment of inflammatory bowel disease. *Gastroenterology* 106, 287–296.
- van Dullemen, H.M., van Deventer, S.J., Hommes, D.W., Bijl, H.A., Jansen, J., Tytgat, G.N., and Woody, J. (1995). Treatment of Crohn's disease with anti-tumor necrosis factor chimeric monoclonal antibody (cA2). *Gastroenterology* 109, 129–135.
- Hata, K., Kazama, S., Nozawa, H., Kawai, K., Kiyomatsu, T., Tanaka, J., Tanaka, T., Nishikawa, T., Yamaguchi, H., Ishihara, S., et al. (2015). Laparoscopic surgery for ulcerative colitis: a review of the literature. *Surg. Today* 45, 933–938.
- Colvin, H., Mizushima, T., Eguchi, H., Takiguchi, S., Doki, Y., and Mori, M. (2017). Gastroenterological surgery in Japan: The past, the present and the future. *Ann Gastroenterol Surg* 1, 5–10.
- Satsangi, J., Parkes, M., Louis, E., Hashimoto, L., Kato, N., Welsh, K., Terwilliger, J.D., Lathrop, G.M., Bell, J.I., and Jewell, D.P. (1996). Two stage genome-wide search in inflammatory bowel disease provides evidence for susceptibility loci on chromosomes 3, 7 and 12. *Nat. Genet.* 14, 199–202.



11. Ng, S.C., Bernstein, C.N., Vatn, M.H., Lakatos, P.L., Loftus, E.V., Jr., Tysk, C., O'Morain, C., Moum, B., and Colombel, J.F.; Epidemiology and Natural History Task Force of the International Organization of Inflammatory Bowel Disease (IOIBD) (2013). Geographical variability and environmental risk factors in inflammatory bowel disease. *Gut* 62, 630–649.
12. He, L., and Hannon, G.J. (2004). MicroRNAs: small RNAs with a big role in gene regulation. *Nat. Rev. Genet.* 5, 522–531.
13. Coskun, M., Bjerrum, J.T., Seidelin, J.B., and Nielsen, O.H. (2012). MicroRNAs in inflammatory bowel disease—pathogenesis, diagnostics and therapeutics. *World J. Gastroenterol.* 18, 4629–4634.
14. Fasseu, M., Tréton, X., Guichard, C., Pedruzzi, E., Cazals-Hatem, D., Richard, C., Aparicio, T., Daniel, F., Soulé, J.C., Moreau, R., et al. (2010). Identification of restricted subsets of mature microRNA abnormally expressed in inactive colonic mucosa of patients with inflammatory bowel disease. *PLoS ONE* 5, e13160.
15. Iborra, M., Bernuzzi, F., Invernizzi, P., and Danese, S. (2012). MicroRNAs in autoimmunity and inflammatory bowel disease: crucial regulators in immune response. *Autoimmun. Rev.* 11, 305–314.
16. Dalal, S.R., and Kwon, J.H. (2010). The Role of MicroRNA in Inflammatory Bowel Disease. *Gastroenterol. Hepatol. (N. Y.)* 6, 714–722.
17. Nguyen, H.T., Dalmasso, G., Yan, Y., Laroui, H., Dahan, S., Mayer, L., Sitaraman, S.V., and Merlin, D. (2010). MicroRNA-7 modulates CD98 expression during intestinal epithelial cell differentiation. *J. Biol. Chem.* 285, 1479–1489.
18. Zhang, Y., Wang, Z., and Gemeinhart, R.A. (2013). Progress in microRNA delivery. *J. Control. Release* 172, 962–974.
19. van Rooij, E., and Kauppinen, S. (2014). Development of microRNA therapeutics is coming of age. *EMBO Mol. Med.* 6, 851–864.
20. Grillone, L.R., and Lanz, R. (2001). Fomivirsen. *Drugs Today (Barc)* 37, 245–255.
21. Gragoudas, E.S., Adamis, A.P., Cunningham, E.T., Jr., Feinsod, M., and Guyer, D.R.; VEGF Inhibition Study in Ocular Neovascularization Clinical Trial Group (2004). Pegaptanib for neovascular age-related macular degeneration. *N. Engl. J. Med.* 351, 2805–2816.
22. Raal, F.J., Santos, R.D., Blom, D.J., Marais, A.D., Charng, M.J., Cromwell, W.C., Lachmann, R.H., Gaudet, D., Tan, J.L., Chasan-Taber, S., et al. (2010). Mipomersen, an apolipoprotein B synthesis inhibitor, for lowering of LDL cholesterol concentrations in patients with homozygous familial hypercholesterolaemia: a randomised, double-blind, placebo-controlled trial. *Lancet* 375, 998–1006.
23. Lim, K.R., Maruyama, R., and Yokota, T. (2017). Eteplirsen in the treatment of Duchenne muscular dystrophy. *Drug Des. Devel. Ther.* 11, 533–545.
24. Brain, O., Owens, B.M.J., Pichulik, T., Allan, P., Khatamzas, E., Leslie, A., Steevens, T., Sharma, S., Mayer, A., Catunescu, A.M., et al. (2013). The intracellular sensor NOD2 induces microRNA-29 expression in human dendritic cells to limit IL-23 release. *Immunity* 39, 521–536.
25. Schmitt, M.J., Margue, C., Behrmann, I., and Kreis, S. (2013). MiRNA-29: a microRNA family with tumor-suppressing and immune-modulating properties. *Curr. Mol. Med.* 13, 572–585.
26. Wu, X., Yamamoto, H., Nakanishi, H., Yamamoto, Y., Inoue, A., Tei, M., Hirose, H., Uemura, M., Nishimura, J., Hata, T., et al. (2015). Innovative delivery of siRNA to solid tumors by super carbonate apatite. *PLoS ONE* 10, e0116022.
27. Takeyama, H., Yamamoto, H., Yamashita, S., Wu, X., Takahashi, H., Nishimura, J., Haraguchi, N., Miyake, Y., Suzuki, R., Murata, K., et al. (2014). Decreased miR-340 expression in bone marrow is associated with liver metastasis of colorectal cancer. *Mol. Cancer Ther.* 13, 976–985.
28. Hiraki, M., Nishimura, J., Takahashi, H., Wu, X., Takahashi, Y., Miyo, M., Nishida, N., Uemura, M., Hata, T., Takemasa, I., et al. (2015). Concurrent Targeting of KRAS and AKT by MiR-4689 Is a Novel Treatment Against Mutant KRAS Colorectal Cancer. *Mol. Ther. Nucleic Acids* 4, e231.
29. Ogawa, H., Wu, X., Kawamoto, K., Nishida, N., Konno, M., Koseki, J., Matsui, H., Noguchi, K., Gotoh, N., Yamamoto, T., et al. (2015). MicroRNAs Induce Epigenetic Reprogramming and Suppress Malignant Phenotypes of Human Colon Cancer Cells. *PLoS ONE* 10, e0127119.
30. Takahashi, H., Nishimura, J., Kagawa, Y., Kano, Y., Takahashi, Y., Wu, X., Hiraki, M., Hamabe, A., Konno, M., Haraguchi, N., et al. (2015). Significance of Polypyrimidine Tract-Binding Protein 1 Expression in Colorectal Cancer. *Mol. Cancer Ther.* 14, 1705–1716.
31. Inoue, A., Mizushima, T., Wu, X., Okuzaki, D., Kambara, N., Ishikawa, S., Wang, J., Qian, Y., Hirose, H., Yokoyama, Y., et al. (2018). A miR-29b Byproduct Sequence Exhibits Potent Tumor-Suppressive Activities via Inhibition of NF- $\kappa$ B Signaling in KRAS-Mutant Colon Cancer Cells. *Mol. Cancer Ther.* 17, 977–987.
32. Tomita, T., Kanai, T., Fujii, T., Nemoto, Y., Okamoto, R., Tsuchiya, K., Totsuka, T., Sakamoto, N., Akira, S., and Watanabe, M. (2008). MyD88-dependent pathway in T cells directly modulates the expansion of colitogenic CD4+ T cells in chronic colitis. *J. Immunol.* 180, 5291–5299.
33. Ozaki, K., Makino, H., Aoki, M., Miyake, T., Yasumasa, N., Osako, M.K., Nakagami, H., Rakugi, H., and Morishita, R. (2012). Therapeutic effect of ribbon-type nuclear factor- $\kappa$ B decoy oligonucleotides in a rat model of inflammatory bowel disease. *Curr. Gene Ther.* 12, 484–492.
34. Bell, S.J., Rigby, R., English, N., Mann, S.D., Knight, S.C., Kamm, M.A., and Stagg, A.J. (2001). Migration and maturation of human colonic dendritic cells. *J. Immunol.* 166, 4958–4967.
35. Becker, C., Wirtz, S., Blessing, M., Pirhonen, J., Strand, D., Bechthold, O., Frick, J., Galle, P.R., Autenrieth, I., and Neurath, M.F. (2003). Constitutive p40 promoter activation and IL-23 production in the terminal ileum mediated by dendritic cells. *J. Clin. Invest.* 112, 693–706.
36. Sarra, M., Pallone, F., Macdonald, T.T., and Monteleone, G. (2010). IL-23/IL-17 axis in IBD. *Inflamm. Bowel Dis.* 16, 1808–1813.
37. Gálvez, J. (2014). Role of Th17 Cells in the Pathogenesis of Human IBD. *ISRN Inflamm.* 2014, 928461.
38. Peer, D., Park, E.J., Morishita, Y., Carman, C.V., and Shimaoka, M. (2008). Systemic leukocyte-directed siRNA delivery revealing cyclin D1 as an anti-inflammatory target. *Science* 319, 627–630.
39. Guo, J., Jiang, X., and Gui, S. (2016). RNA interference-based nanosystems for inflammatory bowel disease therapy. *Int. J. Nanomedicine* 11, 5287–5310.
40. Kriegel, C., and Amiji, M.M. (2011). Dual TNF- $\alpha$ /Cyclin D1 Gene Silencing With an Oral Polymeric Microparticle System as a Novel Strategy for the Treatment of Inflammatory Bowel Disease. *Clin. Transl. Gastroenterol.* 2, e2.
41. Xiao, B., Laroui, H., Viennois, E., Ayyadurai, S., Charania, M.A., Zhang, Y., Zhang, Z., Baker, M.T., Zhang, B., Gewirtz, A.T., and Merlin, D. (2014). Nanoparticles with surface antibody against CD98 and carrying CD98 small interfering RNA reduce colitis in mice. *Gastroenterology* 146, 1289–1300.e1–19.
42. Kennedy, B.W. (2015). Mogensen, an Oral SMAD7 Antisense Oligonucleotide, and Crohn's Disease. *N. Engl. J. Med.* 372, 2461.
43. Seiderer, J., Elben, I., Diegelmann, J., Glas, J., Stallhofer, J., Tillack, C., Pfennig, S., Jürgens, M., Schmechel, S., Konrad, A., et al. (2008). Role of the novel Th17 cytokine IL-17F in inflammatory bowel disease (IBD): upregulated colonic IL-17F expression in active Crohn's disease and analysis of the IL17F p.His161Arg polymorphism in IBD. *Inflamm. Bowel Dis.* 14, 437–445.
44. Ogino, T., Nishimura, J., Barman, S., Kayama, H., Uematsu, S., Okuzaki, D., Osawa, H., Haraguchi, N., Uemura, M., Hata, T., et al. (2013). Increased Th17-inducing activity of CD14+ CD163 low myeloid cells in intestinal lamina propria of patients with Crohn's disease. *Gastroenterology* 145, 1380–1391.e1.
45. Tamai, K., Mizushima, T., Wu, X., Inoue, A., Ota, M., Yokoyama, Y., Miyoshi, N., Haraguchi, N., Takahashi, H., Nishimura, J., et al. (2018). Photodynamic Therapy Using Indocyanine Green Loaded on Super Carbonate Apatite as Minimally Invasive Cancer Treatment. *Mol. Cancer Ther.* 17, 1613–1622.
46. Haccin-Bey-Abina, S., Hauer, J., Lim, A., Picard, C., Wang, G.P., Berry, C.C., Martinache, C., Rieux-Laucat, F., Latour, S., Belohradsky, B.H., et al. (2010). Efficacy of gene therapy for X-linked severe combined immunodeficiency. *N. Engl. J. Med.* 363, 355–364.
47. Inoue, A., Yamamoto, H., Uemura, M., Nishimura, J., Hata, T., Takemasa, I., Ikenaga, M., Ikeda, M., Murata, K., Mizushima, T., et al. (2015). MicroRNA-29b is a Novel Prognostic Marker in Colorectal Cancer. *Ann. Surg. Oncol.* 22 (Suppl 3), S1410–S1418.

48. Wu, Y., Crawford, M., Mao, Y., Lee, R.J., Davis, I.C., Elton, T.S., Lee, L.J., and Nana-Sinkam, S.P. (2013). Therapeutic Delivery of MicroRNA-29b by Cationic Lipoplexes for Lung Cancer. *Mol. Ther. Nucleic Acids* 2, e84.
49. Garzon, R., Heaphy, C.E., Havelange, V., Fabbri, M., Volinia, S., Tsao, T., Zanesi, N., Kornblau, S.M., Marcucci, G., Calin, G.A., et al. (2009). MicroRNA 29b functions in acute myeloid leukemia. *Blood* 114, 5331–5341.
50. Zhao, J.J., Lin, J., Lwin, T., Yang, H., Guo, J., Kong, W., Dessureault, S., Moscinski, L.C., Reznia, D., Dalton, W.S., et al. (2010). microRNA expression profile and identification of miR-29 as a prognostic marker and pathogenetic factor by targeting CDK6 in mantle cell lymphoma. *Blood* 115, 2630–2639.
51. Mott, J.L., Kobayashi, S., Bronk, S.F., and Gores, G.J. (2007). mir-29 regulates Mcl-1 protein expression and apoptosis. *Oncogene* 26, 6133–6140.
52. Qi, Y., Huang, Y., Pang, L., Gu, W., Wang, N., Hu, J., Cui, X., Zhang, J., Zhao, J., Liu, C., et al. (2017). Prognostic value of the MicroRNA-29 family in multiple human cancers: A meta-analysis and systematic review. *Clin. Exp. Pharmacol. Physiol.* 44, 441–454.
53. Wu, F., Zikusoka, M., Trindade, A., Dassopoulos, T., Harris, M.L., Bayless, T.M., Brant, S.R., Chakravarti, S., and Kwon, J.H. (2008). MicroRNAs are differentially expressed in ulcerative colitis and alter expression of macrophage inflammatory peptide-2 alpha. *Gastroenterology* 135, 1624–1635.e24.
54. Nijhuis, A., Biancheri, P., Lewis, A., Bishop, C.L., Giuffrida, P., Chan, C., Feakins, R., Poulosom, R., Di Sabatino, A., Corazza, G.R., et al. (2014). In Crohn's disease fibrosis-reduced expression of the miR-29 family enhances collagen expression in intestinal fibroblasts. *Clin. Sci. (Lond.)* 127, 341–350.